Smearing of the quantum anomalous Hall effect due to statistical fluctuations of magnetic dopants

Z. Yue and M. E. Raikh
Department of Physics and Astronomy, University of Utah, Salt Lake City, Utah 84112, USA
(Received 23 June 2016; published 31 October 2016)

The quantum anomalous Hall effect is induced by substitution of a certain portion x of Bi atoms in a BiTe-based insulating parent compound by magnetic ions (Cr or V). We find the density of in-gap states $N(E)$ emerging as a result of statistical fluctuations of the composition x in the vicinity of the transition point where the *average* gap $\overline{E}_g$ passes through zero. A local gap follows the fluctuations of x. Using the instanton approach, we show that, near the gap edges, the tails are exponential $\ln N(E) \propto -(\overline{E}_g - |E|)$ and the tail states are due to small local gap reduction. Our main finding is that, even when the smearing magnitude exceeds the gap width, there exists a semihard gap around zero energy, where $\ln N(E) \propto -\frac{\overline{E}_g}{|E|}\ln(\frac{\overline{E}_g}{|E|})$. The states responsible for $N(E)$ originate from local gap reversals within narrow rings. The consequence of the semihard gap is the Arrhenius, rather than variable-range hopping, temperature dependence of the diagonal conductivity at low temperatures.

DOI: 10.1103/PhysRevB.94.155313

I. INTRODUCTION

Pairs of spin-degenerate chiral edge modes are implicit for insulators with inverted band structures [1–3]. The minimal model [2] which captures these modes is a 4×4 matrix Hamiltonian acting in the basis of two spin and two orbital states.

The origin of the quantum anomalous Hall (QAH) effect [4] is breaking of the time-reversal symmetry induced by magnetic order. As a result, the symmetry between the two counterpropagating modes at the sample edges is lifted. With a single chiral mode per edge, the Hall conductance of the sample becomes nonzero, and the transport resembles the conventional quantum Hall effect. Experimental studies [5–20] on Cr-doped and V-doped layers of BiTe-based insulating compounds confirm both the quantization of the Hall resistance and the edge transport which accompany the buildup of the magnetic order. Remarkably, resistance jumps observed in Ref. [20] allow for monitoring the switching of magnetization. The common feature of the data reported so far is that the resistance exhibits Arrhenius behavior down to very low temperatures.

For the QAH effect to be pronounced, the bulk of the sample should be strongly insulating. On the other hand, the crossover between a trivial and "topological" band structures takes place as the gap passes through zero. Obviously, the smaller the gap, the easier it is washed out by the disorder. More precisely, the disorder gives rise to in-gap states. However, in the QAH effect, the disorder is of a special type: Randomness in the positions of magnetic ions causes the local fluctuations of the gap *width*. For such fluctuations the energies near the gap center remain unaffected. This is probably the reason why a robust QAH effect is observed in experiments of several groups.

In the present paper we study quantitatively the smearing of the gap due to statistical, and thus unavoidable, magnetic disorder. We find that the states near the gap center are due to the local reversals of the gap *sign* within narrow rings. By employing the instanton approach [21,22] we specify the shape of these fluctuations and the likelihood of their occurrence, which determines the density of the in-gap states. This density of states exhibits a semihard gap near zero energy.

II. INSTANTON APPROACH

Due to the composition disorder, the local value of x, which is the portion of magnetic ions, differs from the average,

$$x(\mathbf{r}) = \overline{x} + \delta x(\mathbf{r}). \tag{1}$$

Fluctuations $\delta x(\mathbf{r})$ are Gaussian with a zero correlation radius,

$$\langle \delta x(\mathbf{r}) \delta x(\mathbf{r}') \rangle = \frac{\overline{x}(1-\overline{x})}{N_0} \delta(\mathbf{r} - \mathbf{r}'), \tag{2}$$

where N_0 is the concentration of Bi lattice sites in which the substitution magnetic ions reside. It is natural to assume that the local gap fluctuations $\Delta(\mathbf{r})$ are proportional to δx, i.e.,

$$\Delta(\mathbf{r}) = E_g(\mathbf{r}) - \overline{E}_g = \alpha\, \delta x(\mathbf{r}), \qquad \alpha = \frac{d\overline{E}_g}{d\overline{x}}. \tag{3}$$

It follows from Eq. (3) that the probability to find the fluctuation $\Delta(\mathbf{r})$ is given by

$$\mathcal{P}\{\Delta(\mathbf{r})\} \propto \exp\left[-\frac{1}{2\gamma}\int d\mathbf{r}\, \Delta^2(\mathbf{r})\right]. \tag{4}$$

where $\gamma = \frac{\alpha^2}{N_0}\overline{x}(1-\overline{x})$.

According to the instanton approach [21,22], the density of states with energy E corresponds to the maximum of the functional $\mathcal{P}$ among all the fluctuations that create a level with energy E. In application to the QAH effect, the wave function $\Psi(\mathbf{r})$, corresponding to this level, is a two-component spinor,

$$\Psi(\mathbf{r}) = \begin{pmatrix} \psi_e(\mathbf{r}) \\ \psi_h(\mathbf{r}) \end{pmatrix}, \tag{5}$$

which satisfies the Schrödinger equation,

$$\hat{h}_{\Delta(\mathbf{r})}\Psi = E\Psi. \tag{6}$$

The Hamiltonian $\hat{h}_{\Delta(\mathbf{r})}$ is a standard Hamiltonian of the minimal model Ref. [2] in which only one spin component is retained. In conventional notations [2] it has the form

$$\hat{h}_{\Delta(\mathbf{r})} = A(\hat{k}_x\sigma_x + \hat{k}_y\sigma_y) + [B\hat{k}^2 + \overline{E}_g + \Delta(\mathbf{r})]\sigma_z, \tag{7}$$

where σ_x, σ_y, and σ_z are the Pauli matrices acting in the pseudospin space. The relative sign of $\overline{E}_g$ and parameter B

determines whether or not the chiral modes are the eigenstates of this Hamiltonian in the presence of an edge [4].

The procedure of minimization of the functional Eq. (4) with restriction Eq. (6) is conventionally carried out [21,22] by introducing the Lagrange multiplier λ and searching for a minimum of the auxiliary functional,

$$\lambda\langle\Psi|\hat{h}_{\Delta(\mathbf{r})}|\Psi\rangle + \frac{1}{2\gamma}\int d\mathbf{r}\,\Delta^2(\mathbf{r}), \tag{8}$$

with respect to $\Delta(\mathbf{r})$. The minimization yields

$$\Delta(\mathbf{r}) = -\lambda\gamma(|\psi_e(\mathbf{r})|^2 - |\psi_h(\mathbf{r})|^2). \tag{9}$$

The remaining task is to substitute Eq. (9) into the Schrödinger equation, find $\psi_e(\mathbf{r})$, $\psi_h(\mathbf{r})$, substitute them into Eq. (9), and evaluate $\mathcal{P}$ with extremal $\Delta(\mathbf{r})$ defined by Eq. (9).

III. ASYMPTOTIC SOLUTION OF THE INSTANTON EQUATION

Assuming the azimuthal symmetry of $\Delta(\mathbf{r})$, the solutions of Eq. (6) can be classified according to the angular momentum: $\psi_e(\mathbf{r}) = i\psi_e^m(\rho)\exp(im\phi)$, $\psi_h(\mathbf{r}) = \psi_h^m(\rho)\exp[i(m+1)\phi]$, where ρ and ϕ are the radius and the azimuthal angle, respectively. Then the system of equations for $\psi_e^m(\rho)$ and $\psi_h^m(\rho)$ reads

$$\begin{aligned}
&\left\{\overline{E}_g - E - \lambda\gamma\left[\left|\psi_e^m(\rho)\right|^2 - \left|\psi_h^m(\rho)\right|^2\right]\right\}\psi_e^m(\rho) \\
&\quad = A\left(\frac{\partial}{\partial\rho} + \frac{m+1}{\rho}\right)\psi_h^m(\rho), \\
&\left\{\overline{E}_g + E - \lambda\gamma\left[\left|\psi_e^m(\rho)\right|^2 - \left|\psi_h^m(\rho)\right|^2\right]\right\}\psi_h^m(\rho) \\
&\quad = A\left(\frac{\partial}{\partial\rho} - \frac{m}{\rho}\right)\psi_e^m(\rho).
\end{aligned} \tag{10}$$

Here we dropped the term $B\hat{k}^2$ in the Hamiltonian $\hat{h}_{\Delta(\mathbf{r})}$ and will incorporate it later, see Appendix A.

The solution of the system is straightforward when the energy E is close to the band-edge $(\overline{E}_g - E) \ll \overline{E}_g$. Then we have $\psi_h^m \ll \psi_e^m$ so that the system Eq. (10) reduces to a single equation,

$$\frac{A^2}{2\overline{E}_g}\nabla^2\psi_e(\mathbf{r}) + \lambda\gamma[\psi_e(\mathbf{r})]^3 = (\overline{E}_g - E)\psi_e(\mathbf{r}). \tag{11}$$

This is a standard instanton equation for a particle moving in a white-noise random potential [21–24]. The radial size of this instanton is $\sim[\overline{E}_g(\overline{E}_g - E)/A^2]^{-1/2}$. Thus, the integral over $\mathbf{r}$ in Eq. (4) is proportional to $(\overline{E}_g - E)$. The full expression for the density of states in the tail reads

$$N(E) \propto \exp\left[-\kappa_0\left(\frac{A^2}{\gamma}\right)\frac{\overline{E}_g - E}{\overline{E}_g}\right], \tag{12}$$

so that the characteristic tail energy is given by $E_t = \frac{\gamma\overline{E}_g}{A^2}$. The value of the numerical factor $\kappa_0 = 5.8$ was established in Refs. [23,24]. It originates from the solution of Eq. (11) with zero angular momentum. Physically, the tail states are due to local gap reductions as depicted in Fig. 1.

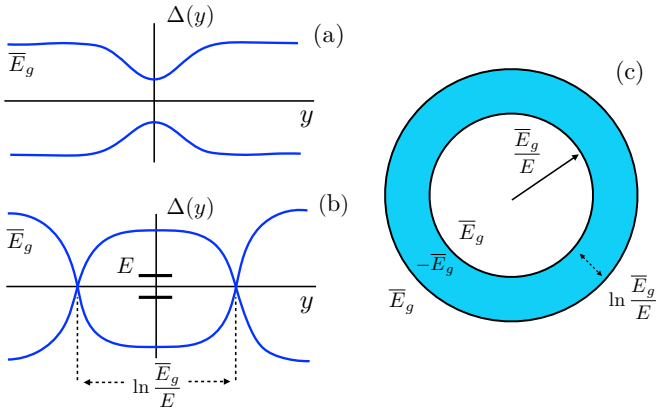

FIG. 1. (a) Fluctuation states near the gap edges are due to local reductions of the width of the gap caused by the composition disorder. (b) To create an in-gap state with energy E, much smaller than the gap width in one-dimensional *two* local gap reversals are required. (c) In two dimensions, the angular motion tends to shift the fluctuation levels away from the gap center. Thus, the fluctuation, responsible for state E, represents a narrow ring of gap reversals with radius $\propto \overline{E}_g/E$.

The result Eq. (12) applies when the tail energy is much smaller than the gap, i.e., for $\gamma \ll A^2$. This result cannot be used even as an order-of-magnitude estimate for the middle of the gap. This is because the shape of the fluctuation $\Delta(\mathbf{r})$ at $|E| \ll \overline{E}_g$ is dramatically different from a simple gap reduction $\Delta(\mathbf{r})$, captured by Eq. (11). Below we demonstrate that for $|E| \ll \overline{E}_g$ the expression for the density of states has the form

$$N(E) \propto \exp\left[-\kappa_1\left(\frac{A^2}{\gamma}\right)\frac{\overline{E}_g}{|E|}\ln\frac{\overline{E}_g}{|E|}\right]. \tag{13}$$

Singular energy dependence of $|\ln\ N(E)|$ reflects the fact that the probability of the formation of a state near the gap center is highly unlikely since the corresponding fluctuation requires a local gap reversal.

To create a state exactly at $E = 0$ the gap should be negative in the left half-space and positive in the right half-space [25] (or vice versa). Naturally, such a fluctuation has a zero probability. To have a finite probability, the fluctuation must include two gap reversals, i.e., $|\Delta(\mathbf{r})|$ should exceed $\overline{E}_g$ inside the fluctuation. To establish the shape of this fluctuation, we start from a one-dimensional case when $|\Delta(\mathbf{r})|$ changes only along the coordinate y, Fig. 1.

A one-dimensional version of the system Eq. (10) reads

$$\begin{aligned}
\{\overline{E}_g - E - \lambda\gamma[|\psi_e(y)|^2 - |\psi_h(y)|^2]\}\psi_e(y) &= A\frac{d\psi_h(y)}{dy}, \\
\{\overline{E}_g + E - \lambda\gamma[|\psi_e(y)|^2 - |\psi_h(y)|^2]\}\psi_h(y) &= A\frac{d\psi_e(y)}{dy}.
\end{aligned} \tag{14}$$

Upon a natural rescaling,

$$y = \frac{A}{\overline{E}_g}\chi, \qquad \varepsilon = \frac{E}{\overline{E}_g}, \qquad \psi_{e,h} = \left(\frac{\overline{E}_g}{\lambda\gamma}\right)^{1/2}\Phi_{e,h}, \tag{15}$$

it acquires a fully dimensionless form

$$\{1-\varepsilon-[|\Phi_e(\chi)|^2-|\Phi_h(\chi)|^2]\}\Phi_e(\chi)=\frac{d\Phi_h}{d\chi},$$
$$\{1+\varepsilon-[|\Phi_e(\chi)|^2-|\Phi_h(\chi)|^2]\}\Phi_h(\chi)=\frac{d\Phi_e}{d\chi}. \tag{16}$$

The dimensionless length in Eq. (16) corresponds to a physical decay length of the wave function in the middle of the gap. Local gap reversals correspond to the regions of χ where $[|\Phi_e(\chi)|^2-|\Phi_h(\chi)|^2]$ exceed 1. A formal reason why there are no midgap fluctuation states is that for $\varepsilon=0$ electron-hole symmetry requires $|\Phi_e(\chi)|^2=|\Phi_h(\chi)|^2$, which is incompatible with the decay of $\Phi_{e,h}$ at $\chi\to\pm\infty$.

To find an asymptotic solution of the system at finite energy, we make use of the smallness of parameter ε. As the first step, instead of Φ_e and Φ_h, we introduce new functions,

$$\Phi_e(\chi)=C(\chi)\cosh\varphi(\chi),\qquad \Phi_h(\chi)=-C(\chi)\sinh\varphi(\chi), \tag{17}$$

after which the system takes the form

$$1-\varepsilon-C(\chi)^2=-\left[\frac{d\varphi}{d\chi}+\tanh\varphi(\chi)\left(\frac{dC}{Cd\chi}\right)\right],$$
$$1+\varepsilon-C(\chi)^2=-\left[\frac{d\varphi}{d\chi}+\frac{1}{\tanh\varphi(\chi)}\left(\frac{dC}{Cd\chi}\right)\right]. \tag{18}$$

Upon subtracting the two equations, we can express the function $C(\chi)$ in terms of $\varphi(\chi)$ as follows:

$$C(\chi)=C_0\exp\left[-\varepsilon\int_0^\chi d\chi'\sinh 2\varphi(\chi')\right], \tag{19}$$

where C_0 is a constant. Substituting this expression back into the system, we arrive at a closed differential-integral equation for $\varphi(\chi)$,

$$1-C_0^2\exp\left[-2\varepsilon\int_0^\chi d\chi'\sinh 2\varphi(\chi')\right]=-\frac{d\varphi}{d\chi}+\varepsilon\cosh 2\varphi. \tag{20}$$

In a zero order in $\varepsilon\ll 1$ the solution of Eq. (20) is a linear function,

$$\varphi(\chi)=\frac{\chi}{b},\qquad b=\frac{1}{C_0^2-1}. \tag{21}$$

Gap reversal, which corresponds to $C_0>1$, is terminated at a certain distance of $\chi=\chi_\varepsilon$ when $\varepsilon\cosh\varphi$ becomes big. This yields

$$\chi_\varepsilon=\frac{b}{2}|\ln\varepsilon|. \tag{22}$$

Importantly, the exponential term on the left-hand side of Eq. (20) drops abruptly from 1 to 0 at the same $\chi=\chi_\varepsilon$, or, more precisely, in the domain $|\chi-\chi_\varepsilon|\lesssim 1$.

The behavior of $C(\chi)$ at $|\chi-\chi_\varepsilon|>1$ can be found by taking into account that the C_0^2 term in Eq. (20) is negligible in this domain. Then it follows from Eq. (20) that the function $\varphi(\chi)$ saturates at the value of $\varphi=\varphi_\varepsilon$ such that $\varepsilon\cosh 2\varphi_\varepsilon=1$. Smallness of ε allows simplifying φ_ε to $\frac{1}{2}|\ln\varepsilon|$. This is exactly the same value which one obtains upon substituting χ_ε into

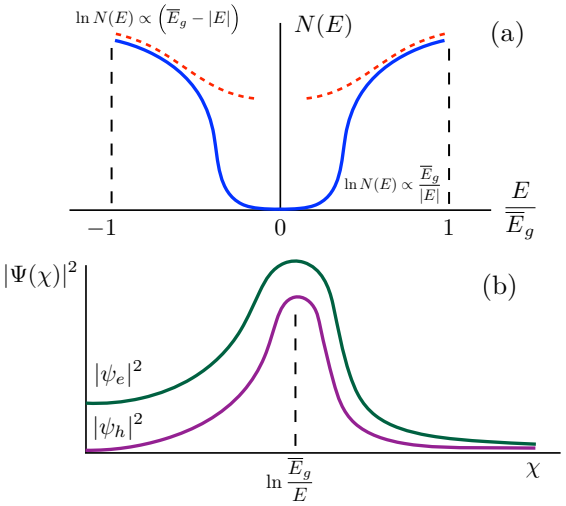

FIG. 2. (a) The density of the in-gap states due to the composition disorder is shown schematically. Near the gap edges (the dashed lines) it is a simple exponent, see Eq. (12), whereas near $E=0$ it represents a semihard gap Eq. (13). (b) The components ψ_e and ψ_h of the spinor corresponding to the fluctuation state $E\ll\overline{E}_g$ are shown schematically versus the dimensionless distance from the ring center. Analytically, ψ_e is given by Eq. (23). The width of the ring exceeds logarithmically the in-gap decay length at $E=0$.

Eq. (21). The fact that $\varphi(\chi)$ saturates at $\chi>\chi_\varepsilon$ suggests that the function $C(\chi)$ falls off exponentially as $\exp[-(\chi-\chi_\varepsilon)]$ at $\chi>\chi_\varepsilon$ as follows from Eq. (19). The behavior of $\varphi(\chi)$ and $C(\chi)$ is depicted in Fig. 2.

Returning to dimensional units, we summarize our result,

$$\Phi_e(y)=\left[\frac{\overline{E}_g}{\lambda\gamma}\left(1+\frac{1}{b}\right)\right]^{1/2}\times\begin{cases}\cosh\left(\frac{\overline{E}_g}{Ab}y\right), & y<y_E,\\ \left(\frac{\overline{E}_g}{E}\right)^{1/2}\exp\left[-\frac{\overline{E}_g}{A}(y-y_E)\right], & y>y_E,\end{cases} \tag{23}$$

where

$$y_E=\frac{A}{\overline{E}_g}\chi_\varepsilon=\frac{Ab}{2\overline{E}_g}\ln\frac{\overline{E}_g}{E}. \tag{24}$$

The corresponding expression for ψ_h differs by replacement of cosh by sinh. At $y=y_E$ the two expressions match within a numerical factor.

The solution Eq. (23) of the system of instanton equations in 1D is, actually, sufficient to find the 2D density of states. Compared to the system Eq. (14), the 2D instanton equations contain the extra "centrifugal" terms $\propto 1/\rho$. These terms create an energy shift of $\sim A/\rho$ and thus prevent the formation of the fluctuation in-gap levels with small energies. For such levels to exist, the double reversal of the gap sign should take place within a ring with radius ρ_E, much bigger than the width, see Fig. 1. Then the solutions of the system Eq. (14) near the ring center are *one dimensional* with $y=\rho-\rho_E$. More quantitatively, see Appendix B, with angular motion taken into account, the energy levels of the ring-shape fluctuation

are given by

$$E_m = \pm\left[A^2\left(\frac{2m+1}{\rho_E}\right)^2 + E^2\right]^{1/2}, \tag{25}$$

where the first term described the quantization of the angular kinetic energy. The above equation suggests that, for level E to exist, the minimal radius of the ring is $A/|E|$.

In the expression Eq. (4) for the density of states the integral $d\mathbf{r}$ can be replaced by the integral $2\pi\rho_E dy$ over the area of the ring,

$$N(E) \propto \exp\left[-\frac{1}{2\gamma}\left(2\pi\rho_E\int_{-\infty}^{\infty} dy\,\Delta^2(y)\right)\right]. \tag{26}$$

The expression for magnitude of the fluctuation $\Delta(y)$ is given by Eq. (9). Taking into account that the dominant contribution to the integral over y comes from the domain $|y| < y_E$, we get

$$N(E) \propto \exp\left[-2\pi\lambda^2\gamma\rho_E\int_0^{y_E} dy\left[\psi_e^2(y) - \psi_h^2(y)\right]^2\right]. \tag{27}$$

Substituting Eq. (23) into Eq. (26) and taking into account that the difference $(\psi_e^2 - \psi_h^2)$ is constant for $y < y_E$, we reproduce the result Eq. (13) in which the constant κ_1 should be identified with a combination,

$$\kappa_1(b) = \pi\left(1 + \frac{1}{b}\right)^2 b. \tag{28}$$

The dependence $\kappa_1(b)$ has a minimum at $b = 1$, where it is equal to 4π. The value $b = 1$ corresponds to $C_0 = 2^{1/2}$, which, in turn, means that the most probable fluctuation corresponds to a complete gap reversal, i.e., the gap is equal to $-\overline{E}_g$ at the core of the fluctuation.

IV. DISCUSSION

The main outcome of our study is that, even when the spins of magnetic dopants are fully aligned, the unavoidable statistical fluctuations in their density (alloy disorder [26–29]) smear the gap $\overline{E}_g$. In conventional semiconductor mixed crystals this disorder is known to cause the tail in the optical absorption and even turn a gapless semiconductor into a metal [28]. The degree of smearing is governed by a dimensionless material parameter,

$$\nu = \frac{\gamma}{A^2} = \frac{\overline{x}(1-\overline{x})}{A^2 N_0}\left(\frac{d\overline{E}_g}{d\overline{x}}\right)^2. \tag{29}$$

For $\nu \ll 1$ only a narrow energy interval $|E - \overline{E}_g| \sim \nu\overline{E}_g$ is affected by the disorder, see Eq. (12). As ν exceeds 1, it might seem from Eq. (12) that the gap is completely washed out. However, our result Eq. (13), see also Fig. 2, suggests that, even for strong disorder, there is an almost hard gap near $E = 0$ which exists in the domain $|E| \lesssim \overline{E}_g/\nu$. Probably, see Appendix C, it is this hard gap that governs the temperature dependence of the longitudinal resistance in the experiments [5–20]. The scale of temperatures for the QAH effect is known to be much lower than the Curie temperature. The fact that the bulk gap in the QAH effect is narrow follows most convincingly from Ref. [10] where the strong temperature-dependent deviations from the quantized value of nondiagonal resistance were observed in a high applied external field so that they cannot be accounted for by the domain structure in the sample. Moreover, the analysis in experimental paper Ref. [15] indicates that the low-temperature behavior of the zero-field diagonal conductivity is activational rather than the variable-range hopping, which is consistent with the scenario of a hard gap. To estimate the experimental value of parameter ν we chose $x = 0.1$ as in most experiments, $A = 3$ eV Å (Ref. [4]) and $\alpha = 2.7$ eV (Ref. [30]). With $N_0 = 5 \times 10^{14}$ cm^{-2}, we got $\nu \approx 0.5$, suggesting that statistical disorder is relevant for the QAH effect.

There are two principal issues that complicate quantitative comparison of our predictions with experiment. First, we used the simplest description of electron states based on the Hamiltonian Eq. (7). This Hamiltonian, proposed in Ref. [30], is believed to capture the low-energy excitations after the pseudospin components ψ_e and ψ_h are identified with symmetric and antisymmetric combinations of the top and bottom surface states. However, the experiments were performed on multilayer structures. It is unclear whether the purely 2D description applies to them quantitatively. Second, in realistic samples, the in-gap states due to the magnetic disorder can be masked by the smearing due to nonmagnetic impurities. In-gap states due to these impurities do not "preserve" the energy $E = 0$. The only information about the disorder in the QAH samples is the value of mobility $\mu = 760$ cm^2 V^{-1} s^{-1}, measured in Ref. [8] at a temperature of 80 K, much higher than the Curie temperature of 15 K. However, relating this mobility to the random potential, which could be added to the Hamiltonian Eq. (7), is impossible, again, due to the complex band structure of multilayers.

In conclusion, we point out that for a really strong disorder $\nu \gg 1$, the hard gap near $E = 0$ disappears. In this limit one can neglect $\overline{E}_g$ in the Hamiltonian so that the problem is reduced to disorder-induced smearing of a linear Dirac spectrum. This problem has a long history [31–33] and was addressed in relation to, e.g., d-wave superconductivity. However, in the absence of an energy scale to compare the disorder with, there is no definite answer.

ACKNOWLEDGMENTS

We are grateful to D. A. Pesin for an illuminating discussion on the relevance of the Hamiltonian Eq. (7). We are also grateful to J. Wang (Stanford University) for introducing the topic of the QAH effect to us. This work was supported by the NSF through MRSEC Grant No. DMR-1121252.

APPENDIX A: THE ROLE OF THE Bk^2 TERM IN THE HAMILTONIAN

In order to estimate the effect of the Bk^2 term in the Hamiltonian Eq. (7), we compare it to the linear term and find the scale of momenta $k \sim A/B$ when this term becomes important. In other words, the term Bk^2 plays a dominant role when the spatial scales in the problem are $\sim B/A$. On the other hand, with logarithmic accuracy, the size of the fluctuation is $\sim A/\overline{E}_g$. The ratio of the two scales yields a dimensionless parameter $B\overline{E}_g/A^2$, which becomes progressively small as the

gap decreases. More quantitative information about the role of Bk^2 can be obtained upon incorporating it into Eq. (20). Then it takes the form

$$\frac{d\varphi}{d\chi} = C_0^2 \exp\left[-2\varepsilon \int_0^\chi d\chi' \sinh 2\varphi(\chi')\right] - 1 + \varepsilon \cosh 2\varphi + \frac{B\overline{E}_g}{A^2}\left[\left(\frac{d\varphi}{d\chi}\right)^2 - \frac{d^2\varphi}{d\chi^2}\right]. \tag{A1}$$

Similar to the steps in the main text, we neglect small terms containing ε and substitute $\varphi(\chi) = \chi/b$. This leads to the following modified relation between parameters b and C_0:

$$C_0^2 = 1 + \frac{1}{b} - \left(\frac{B\overline{E}_g}{A^2}\right)\frac{1}{b^2}. \tag{A2}$$

Note that for the topological band structure, when the signs of B and $\overline{E}_g$ are opposite, the last term in Eq. (A2) causes only a slight increase in C_0, which results in a small suppression of the exponent in the density of states. On the contrary, for a trivial band structure, this last term decreases C_0, leading to the enhancement of the density of states. Moreover, Eq. (A2) suggests that this enhancement can be parametrically big when the second and third terms closely compensate each other. For such a compensation the width of the ring should be on the order of the minimal length B/A. This, however, violates our basic assumption that the shape of the fluctuation is dominated by the inner part.

APPENDIX B: QUANTIZED LEVELS ON A RING WITH AN INVERTED BAND GAP

Consider a gap-inverting fluctuation confined to a ring $\rho_1 < \rho < \rho_2$. More specifically, the gap $\Delta(\mathbf{r})$ changes in a radial direction as follows:

$$\Delta(\mathbf{r}) = \begin{cases} \Delta_0, & 0 < \rho < \rho_1, \\ -\Delta_0, & \rho_1 < \rho < \rho_2, \\ \Delta_0, & \rho > \rho_2. \end{cases} \tag{B1}$$

We assume for simplicity that the gap reversal is full. In the domain $\rho < \rho_1$, the in-gap solution of the system Eq. (10) which is finite at the origin reads

$$\begin{pmatrix} \psi_e^m(\rho) \\ \psi_h^m(\rho) \end{pmatrix} = \begin{pmatrix} \alpha I_{m+1}(s\rho) \\ \sqrt{\frac{\Delta_0 - E}{\Delta_0 + E}}\alpha I_m(s\rho) \end{pmatrix}, \tag{B2}$$

where $I_m(z)$ is the modified Bessel function and $s = \frac{\sqrt{\Delta_0^2 - E^2}}{A}$. The corresponding solution for $\rho > \rho_2$, which decays at $\rho \to \infty$ can be expressed in terms of the Macdonald function as follows:

$$\begin{pmatrix} \psi_e^m(\rho) \\ \psi_h^m(\rho) \end{pmatrix} = \begin{pmatrix} \beta K_{m+1}(s\rho) \\ -\sqrt{\frac{\Delta_0 - E}{\Delta_0 + E}}\beta K_m(s\rho) \end{pmatrix}. \tag{B3}$$

Within the ring, the solution is a linear combination of $I_m(s\rho)$ and $K_m(s\rho)$,

$$\begin{pmatrix} \psi_e^m(\rho) \\ \psi_h^m(\rho) \end{pmatrix} = \begin{pmatrix} \alpha_1 I_{m+1}(s\rho) + \beta_1 K_{m+1}(s\rho) \\ \sqrt{\frac{\Delta_0 + E}{\Delta_0 - E}}[-\alpha_1 I_m(s\rho) + \beta_1 K_m(s\rho)] \end{pmatrix}, \tag{B4}$$

The gap inversion is reflected in the relative signs of the components of the spinor inside and outside the ring. Four unknown coefficients, α, β, α_1, and β_1 are related by the continuity of the components of the spinors at $\rho = \rho_1$ and $\rho = \rho_2$. The energy levels are determined from the condition of consistency of the system, which reads

$$\left(\frac{\Delta_0 - E}{\Delta_0 + E}\right)\frac{K_m(s\rho_2)}{K_{m+1}(s\rho_2)} = \frac{\left(I_{m+1}(s\rho_1)K_m(s\rho_1) - \frac{\Delta_0 - E}{\Delta_0 + E} I_m(s\rho_1)K_{m+1}(s\rho_1)\right)I_m(s\rho_2) - \frac{2\Delta_0}{\Delta_0 + E} I_{m+1}(s\rho_1)I_m(s\rho_1)K_m(s\rho_2)}{\left(I_{m+1}(s\rho_1)K_m(s\rho_1) - \frac{\Delta_0 - E}{\Delta_0 + E} I_m(s\rho_1)K_{m+1}(s\rho_1)\right)I_{m+1}(s\rho_2) + \frac{2\Delta_0}{\Delta_0 + E} I_{m+1}(s\rho_1)I_m(s\rho_1)K_{m+1}(s\rho_2)}. \tag{B5}$$

The near-midgap levels with $|E| \ll \Delta_0$ appear only when the conditions $s\rho_1 \gg 1$ and $s(\rho_2 - \rho_1) \gg 1$ are met. Under these conditions Eq. (B5) allows serious simplifications. First, using the asymptotes of the Bessel functions, the common bracket in the numerator and denominator on the right-hand side simplifies to

$$I_{m+1}(s\rho_1)K_m(s\rho_1) - \left(\frac{\Delta_0 - E}{\Delta_0 + E}\right)I_m(s\rho_1)K_{m+1}(s\rho_1) \approx \frac{1}{2s\rho_1}\left(\frac{2E}{\Delta_0} - \frac{2m+1}{s\rho_1}\right). \tag{B6}$$

As the next step, we divide both sides by the ratio $I_m(s\rho_2)/I_{m+1}(s\rho_2)$ and take the large-ρ asymptotes. Then the left-hand side takes the form

$$\left(\frac{\Delta_0 - E}{\Delta_0 + E}\right)\frac{K_m(s\rho_2)I_{m+1}(s\rho_2)}{K_{m+1}(s\rho_2)I_m(s\rho_2)} = 1 - \frac{2E}{\Delta_0} - \frac{2m+1}{s\rho_2}. \tag{B7}$$

The expressions in the numerator and denominator on the right-hand side are equal to Eq. (B6) ± a small correction. The asymptotic form of this correction is the following:

$$\frac{2\Delta_0}{\Delta_0 + E} I_{m+1}(s\rho_1)I_m(s\rho_1)\frac{K_m(s\rho_2)}{I_m(s\rho_2)} \approx \frac{2\Delta_0}{\Delta_0 + E} I_{m+1}(s\rho_1)I_m(s\rho_1)\frac{K_{m+1}(s\rho_2)}{I_{m+1}(s\rho_2)} \approx \frac{2e^{-2s(\rho_2 - \rho_1)}}{2s\rho_1}. \tag{B8}$$

Upon combining Eqs. (B6)–(B8), the equation for the energy levels reduces to

$$1 - \frac{2E}{\Delta_0} - \frac{2m+1}{s\rho_2} = 1 - \frac{4\exp[-2s(\rho_2 - \rho_1)]}{\frac{2E}{\Delta_0} - \frac{2m+1}{s\rho_1}}. \tag{B9}$$

For a narrow ring one can replace ρ_1 and ρ_2 in the denominators by $(\rho_1 + \rho_2)/2$. Also, with accuracy E^2/Δ_0^2, one can replace s

by Δ_0/A. This leads to the following expression for the energy levels:

$$\left(\frac{2E}{\Delta_0}\right)^2 = \left[\frac{2(2m+1)A}{\Delta_0(\rho_1+\rho_2)}\right]^2 + 4\exp\left[-2\frac{(\rho_2-\rho_1)\Delta_0}{A}\right]. \tag{B10}$$

The right-hand side is the sum of contributions from the quantized motion along the ring and quantized motion across the ring as in Eq. (23).

APPENDIX C: TEMPERATURE DEPENDENCE OF CONDUCTIVITY

Neglecting the energy dependence of the logarithm in Eq. (13), we approximate the energy-dependent density of states with

$$N(E) = N_0 \exp\left(-\frac{\overline{E}_g}{\nu E}\right), \tag{C1}$$

where parameter ν is defined by Eq. (27). Assume that the energy responsible for the transport is E_0. The density of states can be treated as a constant within a strip $|E - E_0| < \nu E_0^2/\overline{E}_g$. A typical distance between the localized states within the strip is

$$r(E_0) = \left(\frac{\nu E_0^2 N(E_0)}{\overline{E}_g}\right)^{-1/2}. \tag{C2}$$

Following the derivation of Mott's law, we minimize the log-resistance,

$$\ln R(E_0) = \frac{E_0}{T} + \frac{2r(E_0)}{\xi}, \tag{C3}$$

corresponding to activation into the strip and tunneling between the neighbors with respect to E_0. Here ξ is the localization radius. The condition of the minimum reads

$$\frac{1}{T} = \frac{1}{(N_0\xi^2)^{1/2}}\left(\frac{\overline{E}_g}{\nu E_0^2}\right)^{3/2}\exp\left(\frac{\overline{E}_g}{2\nu E_0}\right), \tag{C4}$$

where we have differentiated only the exponent in $r(E_0)$. Upon expressing E_0 from Eq. (C4) and substituting it back into Eq. (C3), we find with logarithmic accuracy,

$$\ln R(E_0) = \frac{\overline{E}_g}{2\nu T}\left[\ln\frac{\overline{E}_g}{\nu T}\left(\frac{N_0\xi^2\overline{E}_g}{\nu}\right)^{1/2}\right]^{-1}. \tag{C5}$$

The result Eq. (C5) applies when the logarithm is big. By virtue of the same condition the activation term in Eq. (C4) exceeds the tunneling term. Concerning the dimensionless combination $N_0\xi^2\overline{E}_g$ under the logarithm with localization length $\xi = A/\overline{E}_g$ in the middle of the gap being disorder independent, this combination is some unknown power of ν. Thus, for $\nu \sim 1$, Eq. (C5) applies for $T < \overline{E}_g$. We conclude that, due to a rapid growth of the density of states away from the gap center, the behavior of the resistance remains Arrhenius even at low temperatures. This is consistent with the observation in Ref. [15].

[1] C. L. Kane and E. J. Mele, Phys. Rev. Lett. **95**, 226801 (2005).
[2] B. A. Bernevig, T. L. Hughes, and S.-C. Zhang, Science **314**, 1757 (2006).
[3] B. A. Bernevig and S.-C. Zhang, Phys. Rev. Lett. **96**, 106802 (2006).
[4] C.-X. Liu, X.-L. Qi, X. Dai, Z. Fang, and S.-C. Zhang, Phys. Rev. Lett. **101**, 146802 (2008).
[5] J. G. Checkelsky, J. Ye, Y. Onose, Y. Iwasa, and Y. Tokura, Nat. Phys. **8**, 729 (2012).
[6] C.-Z. Chang, J. Zhang, M. Liu, Z. Zhang, X. Feng, K. Li, L.-L. Wang, X. Chen, X. Dai, Z. Fang, X.-L. Qi, S.-C. Zhang, Y. Wang, K. He, X.-C. Ma, and Q.-K. Xue, Adv. Mater. **25**, 1065 (2013).
[7] X. Kou, M. Lang, Y. Fan, Y. Jiang, T. Nie, J. Zhang, W. Jiang, Y. Wang, Y. Yao, L. He, and K. L. Wang, ACS Nano **7**, 9205 (2013).
[8] C.-Z. Chang, J. Zhang, X. Feng, J. Shen, Z. Zhang, M. Guo, K. Li, Y. Ou, P. Wei, L.-L. Wang, Z.-Q. Ji, Y. Feng, S. Ji, X. Chen, J. Jia, X. Dai, Z. Fang, S.-C. Zhang, K. He, Y. Wang, L. Lu, X.-C. Ma, and Q.-K. Xue, Science **340**, 167 (2013).
[9] J. G. Checkelsky, R. Yoshimi, A. Tsukazaki, K. S. Takahashi, Y. Kozuka, J. Falson, M. Kawasaki, and Y. Tokura, Nat. Phys. **10**, 731 (2014).
[10] X. Kou, S.-T. Guo, Y. Fan, L. Pan, M. Lang, Y. Jiang, Q. Shao, T. Nie, K. Murata, J. Tang, Y. Wang, L. He, T.-K. Lee, W.-L. Lee, and K. L. Wang, Phys. Rev. Lett. **113**, 137201 (2014).
[11] C.-Z. Chang, W. Zhao, D. Y. Kim, H. Zhang, B. A. Assaf, D. Heiman, S.-C. Zhang, C. Liu, M. H. W. Chan, and J. S. Moodera, Nature Mater. **14**, 473 (2015).
[12] A. Kandala, A. Richardella, S. Kempinger, C.-X. Liu, and N. Samarth, Nat. Commun. **6**, 7434 (2015).
[13] M. Mogi, R. Yoshimi, A. Tsukazaki, K. Yasuda, Y. Kozuka, K. S. Takahashi, M. Kawasaki, and Y. Tokura, Appl. Phys. Lett. **107**, 182401 (2015).
[14] X. Kou, L. Pan, J. Wang, Y. Fan, E. S. Choi, W.-L. Lee, T. Nie, K. Murata, Q. Shao, S.-C. Zhang, and K. L. Wang, Nat. Commun. **6**, 8474 (2015).
[15] A. J. Bestwick, E. J. Fox, X. Kou, L. Pan, K. L. Wang, and D. Goldhaber-Gordon, Phys. Rev. Lett. **114**, 187201 (2015).
[16] C.-Z. Chang, W. Zhao, D. Y. Kim, P. Wei, J. K. Jain, C. Liu, M. H. W. Chan, and J. S. Moodera, Phys. Rev. Lett. **115**, 057206 (2015).
[17] S. Grauer, S. Schreyeck, M. Winnerlein, K. Brunner, C. Gould, and L. W. Molenkamp, Phys. Rev. B **92**, 201304(R) (2015).

[18] E. O. Lachman, A. F. Young, A. Richardella, J. Cuppens, H. R. Naren, Y. Anahory, A. Y. Meltzer, A. Kandala, S. Kempinger, Y. Myasoedov, M. E. Huber, N. Samarth, and E. Zeldov, Sci. Adv. **1**, e1500740 (2015).
[19] Y. Feng, X. Feng, Y. Ou, J. Wang, C. Liu, L. Zhang, D. Zhao, G. Jiang, S.-C. Zhang, K. He, X. Ma, Q.-K. Xue, and Y. Wang, Phys. Rev. Lett. **115**, 126801 (2015).
[20] M. Liu, W. Wang, A. R. Richardella, A. Kandala, J. Li, A. Yazdani, N. Samarth, and N. P. Ong, Sci. Adv. **2**, e1600167 (2016).
[21] B. I. Halperin and M. Lax, Phys. Rev. **148**, 722 (1966).
[22] J. Zittartz and J. S. Langer, Phys. Rev. **148**, 741 (1966).
[23] D. J. Thouless and M. E. Elzain, J. Phys. C **11**, 3425 (1978).
[24] E. Brezin and G. Parisi, J. Phys. C **13**, L307 (1980).
[25] A. W. W. Ludwig, M. P. A. Fisher, R. Shankar, and G. Grinstein, Phys. Rev. B **50**, 7526 (1994).
[26] Z. I. Alferov, E. L. Portnoi, and A. A. Rogachev, Sov. Phys. Semicond. **2**, 1001 (1969).
[27] S. D. Baranovskii and A. L. Efros, Sov. Phys. Semicond. **12**, 1328 (1978).
[28] N. N. Ablyazov, M. E. Raikh, and A. L. Efros, Pis'ma Zh. Eksp. Teor. Fiz. **38**, 103 (1983).
[29] A. L. Efros and M. E. Raikh, in *Optical Properties of Mixed Crystals*, edited by R. J. Elliot and I. P. Ipatova (Elsevier Science, Amsterdam, 1988), p. 133.
[30] R. Yu, W. Zhang, H.-J. Zhang, S.-C. Zhang, X. Dai, and Z. Fang, Science **329**, 61 (2010).
[31] M. P. A. Fisher and E. Fradkin, Nucl. Phys. B **251**, 457 (1985).
[32] P. A. Lee, Phys. Rev. Lett. **71**, 1887 (1993).
[33] A. A. Nersesyan, A. M. Tsvelik, and F. Wenger, Phys. Rev. Lett. **72**, 2628 (1994).